

Effects of an embedding bulk fluid on phase separation dynamics in a thin liquid film

S. RAMACHANDRAN¹, S. KOMURA^{1(a)} and G. GOMPPER²

¹ *Department of Chemistry, Graduate School of Science and Engineering, Tokyo Metropolitan University Tokyo 192-0397, Japan*

² *Institut für Festkörperforschung, Forschungszentrum Jülich - D-52425 Jülich, Germany, EU*

received 5 December 2009; accepted in final form 23 February 2010
published online 25 March 2010

PACS 68.05.-n – Liquid-liquid interfaces

PACS 87.16.D- – Membranes, bilayers, and vesicles

PACS 87.16.dp – Transport, including channels, pores, and lateral diffusion

Abstract – Using dissipative-particle-dynamics simulations, we study the effects of an embedding bulk fluid on the phase separation dynamics in a thin planar liquid film. The domain growth exponent is altered from 2D to 3D behavior upon the addition of a bulk fluid, even though the phase separation occurs in 2D geometry. Correlated diffusion measurements in the film show that the presence of bulk fluid changes the nature of the longitudinal coupling diffusion coefficient from logarithmic to algebraic dependence of $1/s$, where s is the distance between the two particles. This result, along with the scaling exponents, suggests that the phase separation takes place through the Brownian coagulation process.

Copyright © EPLA, 2010

Introduction. – Lipid molecules constituting the membranes of biological cells play a major role in the regulation of various cellular processes. About a decade ago Simons and Ikonen proposed a hypothesis which suggests that the lipids organize themselves into sub-micron-sized domains termed “rafts” [1]. The rafts serve as platforms for proteins, which in turn attributes a certain functionality to each domain. Although there have been extensive studies in this area, the details of the underlying physical mechanisms leading to formation of rafts, their stability, and the regulation of their finite domain size remain elusive. Numerous experiments on intact cells and artificial membranes containing mixtures of saturated lipids, unsaturated lipids and cholesterol, have demonstrated the segregation of the lipids into liquid-ordered and liquid-disordered phases [2]. Recent experimental observations of critical fluctuations point towards the idea that the cell maintains its membrane slightly above the critical point [3,4]. Below the transition temperature, there have been studies on the dynamics in multicomponent membranes such as diffusion of domains [5] and domain coarsening [6]. A clear understanding of phase separation may contribute towards a better explanation of the dynamics of lipid organization

in cell membranes. Apart from biological membranes, it is of relevance to understand the dynamics of Langmuir monolayer systems which are also thin fluid films.

Phase separation of binary fluids following a quench has been under study for over forty years [7]. The dynamic scaling hypothesis assumes that there exists a scaling regime characterized by the average domain size R that grows with time t as $R \sim t^\alpha$ with a universal exponent α . For three-dimensional (3D) off-critical binary fluids, there is an initial growth by the Brownian coagulation process [8], followed by the Lifshitz-Slyozov (LS) evaporation-condensation process [9]; both mechanisms show a growth exponent $\alpha = 1/3$. This is followed by a late time inertial regime of $\alpha = 2/3$ [10]. For critical mixtures, there is an intermediate $\alpha = 1$ regime owing to interface diffusion [11]. The scenario is slightly different for pure two-dimensional (2D) systems [12]. For an off-critical mixture, it was predicted that after the initial formation of domains, they grow by the Brownian coagulation mechanism with a different exponent $\alpha = 1/2$ (as will be explained later), followed by a crossover to the LS mechanism which gives $\alpha = 1/3$ even in 2D. For critical mixtures, on the other hand, the initial quench produces an interconnected structure which coarsens and then breaks up due to the interface diffusion with an exponent $\alpha = 1/2$. After the breakup processes, coarsening takes place through

^(a)E-mail: komura@tmu.ac.jp

Brownian coagulation that is again characterized by the $\alpha = 1/2$ scaling [8]. These predictions were confirmed by molecular-dynamics simulations in 2D [13]. The exponent $\alpha = 1/2$ was also observed in 2D lattice-Boltzmann simulations in the presence of thermal noise for a critical mixture [14].

Although biomembranes composed of lipid bilayers can be regarded as 2D viscous fluids, they are not isolated pure 2D systems since lipids are coupled to the adjacent fluid. Hence it is of great interest to investigate the phase separation dynamics in such a quasi-2D liquid film in the presence of hydrodynamic interaction. (We use the word “quasi-2D” whenever the film is coupled to the bulk fluid.) To address this problem, we consider a 2D binary viscous fluid in contact with a bulk fluid. Our approximation of the membrane as a planar 2D liquid film is valid in the limit of large bending rigidity (common in biological membranes) or in the presence of a lateral tension, which both act to suppress membrane undulations. We employ a simple model in which the film is confined to a plane with the bulk fluid particles added above and below. In our model using a dissipative-particle-dynamics (DPD) simulation technique, the exchange of momentum between the film and the bulk fluid is naturally taken into account. We particularly focus on the effect of bulk fluid on the quasi-2D phase separation. We show that the presence of a bulk fluid will alter the domain growth exponent from that of 2D to 3D indicating the significant role played by the film-solvent coupling. In order to elucidate the underlying physical mechanism of this effect, we have looked into the diffusion properties in the film by measuring two-particle correlated diffusion. Our result suggests that quasi-2D phase separation proceeds by the Brownian coagulation mechanism which reflects the 3D nature of the bulk fluid. Such a behavior is universal as long as the domain size exceeds the Saffman-Delbrück length [15].

Model and simulation technique. – For the purpose of our study, we use a structureless model of the 2D liquid film within the DPD framework [16,17]. As shown in fig. 1, the 2D film is represented by a single layer of particles confined to a plane. In order to study phase separation, we introduce two species of particles, *A* and *B*. The bulk fluid which we call as “solvent” (*S*) is also represented by single particles of same size as that of the film particles. All particles have the same mass *m*. We avoid using the existing DPD models for a self-assembling bilayer [18,19] as they inherently include bending and protrusion modes, which makes it difficult to separate hydrodynamic effects from the effect of membrane shape deformations.

In DPD, the interaction between any two particles, within a range r_0 , is linearly repulsive. The pairwise interaction leads to full momentum conservation, which in turn brings out the correct fluid hydrodynamics. The force on a particle *i* is given by

$$m \frac{d\mathbf{v}_i}{dt} = \sum_{j \neq i} [\mathbf{F}_{ij}^C(\mathbf{r}_{ij}) + \mathbf{F}_{ij}^D(\mathbf{r}_{ij}, \mathbf{v}_{ij}) + \mathbf{F}_{ij}^R(\mathbf{r}_{ij})], \quad (1)$$

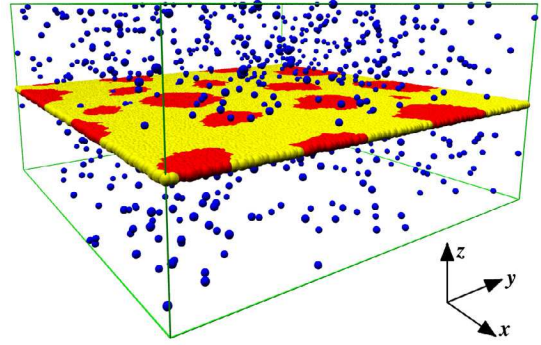


Fig. 1: (Colour on-line) Image of the model film with the bulk fluid called solvent. The yellow and red particles represent the two components constituting the model film, while blue ones represent the solvent. For clarity, only a fraction of the solvent particles are shown.

where $\mathbf{r}_{ij} = \mathbf{r}_i - \mathbf{r}_j$ and $\mathbf{v}_{ij} = \mathbf{v}_i - \mathbf{v}_j$. Of the three types of forces acting on the particles, the conservative force on particle *i* due to *j* is $\mathbf{F}_{ij}^C = a_{ij}\omega(r_{ij})\hat{\mathbf{r}}_{ij}$, where a_{ij} is an interaction strength and $\hat{\mathbf{r}}_{ij} = \mathbf{r}_{ij}/r_{ij}$ with $r_{ij} = |\mathbf{r}_{ij}|$. The second type of force is the dissipative force $\mathbf{F}_{ij}^D = -\Gamma_{ij}\omega^2(r_{ij})(\hat{\mathbf{r}}_{ij} \cdot \mathbf{v}_{ij})\hat{\mathbf{r}}_{ij}$, where Γ_{ij} is the dissipative strength for the pair (*i*, *j*). The last is the random force $\mathbf{F}_{ij}^R = \sigma_{ij}(\Delta t)^{-1/2}\omega(r_{ij})\zeta_{ij}\hat{\mathbf{r}}_{ij}$, where σ_{ij} is the amplitude of the random noise for the pair (*i*, *j*), and ζ_{ij} is a random variable with zero mean and unit variance which is uncorrelated for different pairs of particles and different time steps. The dissipative and random forces act as a thermostat, provided the fluctuation-dissipation theorem $\sigma_{ij}^2 = 2\Gamma_{ij}k_B T$ is satisfied (k_B is Boltzmann constant and *T* is the thermostat temperature). The weight factor is chosen as $\omega(r_{ij}) = 1 - r_{ij}/r_0$ up to the cutoff radius r_0 and zero thereafter. The particle trajectories are obtained by solving eq. (1) using the velocity-Verlet integrator. In the simulation, r_0 and *m* set the scales for length and mass, respectively, while $k_B T$ sets the energy scale. The time is measured in units of $\tau = (mr_0^2/k_B T)^{1/2}$. The numerical value of the amplitude of the random force is assumed to be the same for all pairs such that $\sigma_{ij} = 3.0[(k_B T)^3 m/r_0^2]^{1/4}$, and the fluid density is set as $\rho = 3.0$. We set $k_B T = 1$ and the integration time step is chosen to be $\Delta t = 0.01\tau$.

The thin film is constructed by placing particles in the *xy*-plane in the middle of the simulation box (see fig. 1). Owing to the structureless representation of the constituent particles, we apply an external potential so as to maintain the film integrity. This is done by fixing the *z*-coordinates of all the film particles. It is known that confinement of simulation particles between walls leads to a reduction in the solvent temperature near the wall [20]. However, since we allow for the in-plane motion of the film particles, the solvent temperature is found to be only 2% less than the bulk near the 2D film. Hence we consider that this effect is negligible. Our work involves the systematic

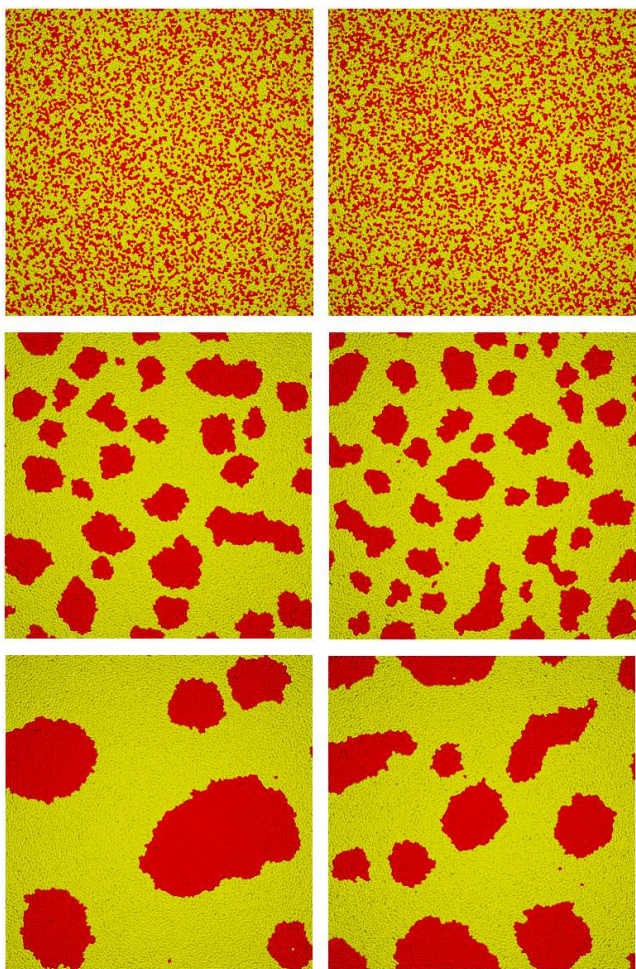


Fig. 2: (Colour on-line) The snapshots for a 70 : 30 mixture (yellow and red) undergoing phase separation at $t = 0, 150$ and 1000 (top to bottom) for a pure 2D (left column) and quasi-2D system with $L_z = 40$ (right column). The above snapshots are from one of the ten independent trials that were conducted.

variation of the height of the simulation box starting from the pure 2D case. In the absence of solvent, we work with a 2D-box of dimensions $L_x \times L_y = 80 \times 80$ with 19200 particles constituting the film. For the quasi-2D studies, we add solvent particles S above and below the model film, and increase the height of the box as $L_z = 5, 20$ and 40 . For all the cases there are 19200 film particles. The largest box size ($L_z = 40$) has 748800 solvent particles. The box with height $L_z = 40$ is found to be sufficiently large enough to prevent the finite-size effect which affects the solvent-film interaction. The system is then subject to periodic boundary conditions in all the three directions. For phase separation simulations, we introduce two species of film particles A and B . The interaction parameter between various particles are given by $a_{AA} = a_{BB} = a_{SS} = a_{AS} = a_{BS} = 25$ and $a_{AB} = 50$. In order to do a quench, the film is first equilibrated with a single component, following which a fraction of the particles are instantaneously changed to the B type.

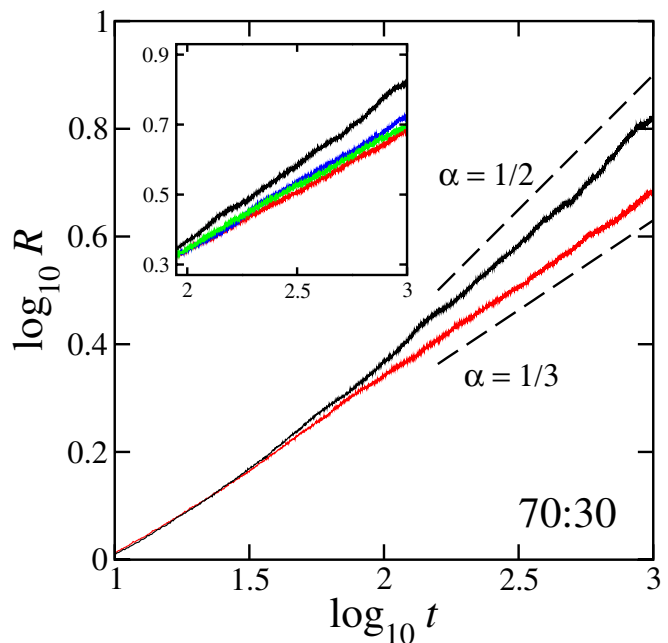


Fig. 3: (Colour on-line) The average domain size R as a function of time t for a 70 : 30 off-critical mixture. The upper black curve is the pure 2D case showing an $\alpha = 1/2$ scaling, and the lower red curve is the quasi-2D case when $L_z = 40$ showing a distinct $\alpha = 1/3$ scaling. The inset shows the zoomed in portion with different box heights in the z -direction, *i.e.*, $L_z = 0, 5, 20$ and 40 starting from the top black curve.

Phase separation. – First we describe the results of the phase separation dynamics. The snapshots for the $A : B$ composition set to 70 : 30 (off-critical mixture) are shown in fig. 2 for both the pure 2D case (left column) and the quasi-2D case with $L_z = 40$ (right column). Qualitatively, it is seen that the domains for the quasi-2D case are smaller in size when compared at the same time step. We also monitor the average domain size $R(t)$ which can be obtained from the total interface length $L(t)$ between the two components. This is because $R(t)$ and $L(t)$ are related by $L(t) = 2\pi N(t)R(t)$, where $N(t)$ is the number of domains. The area occupied by the B -component is given by $\mathcal{A} = \pi N(t)R^2(t)$ which is a conserved quantity. Then we have

$$R(t) = 2\mathcal{A}/L(t). \quad (2)$$

When the domain size grows as $R \sim t^\alpha$, one has $L \sim t^{-\alpha}$ and $N \sim t^{-2\alpha}$. The domain size $R(t)$ for a 70 : 30 mixture is shown in fig. 3. In this plot, the average over 10 independent trials has been taken. It can be seen that the pure 2D case has a growth exponent $\alpha = 1/2$. Upon the addition of solvent, we observe that the exponent shifts to a lower value of $\alpha = 1/3$. This exponent is reminiscent of the phase separation dynamics of an off-critical mixture in 3D. Upon systematically increasing the amount of solvent in the system by changing the height L_z , we can see a clear deviation from the pure 2D behavior (see the inset of fig. 3). There is no further change if L_z is increased beyond 40. We note that the scaling regime

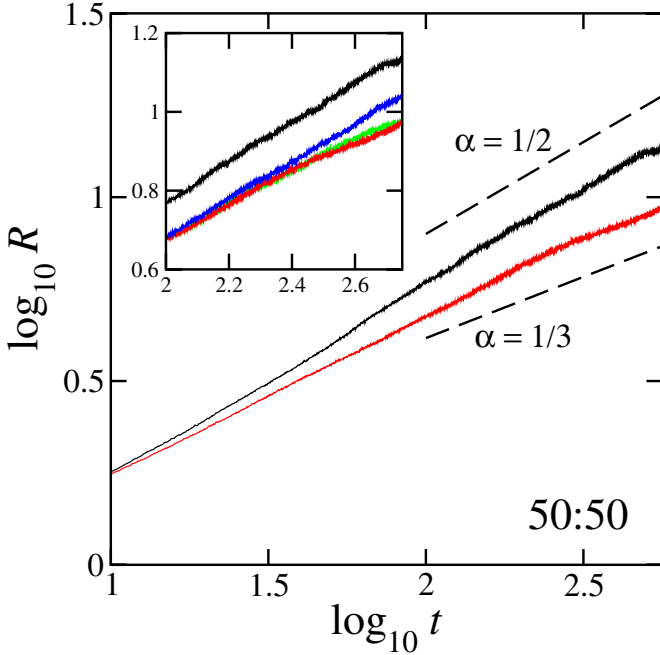


Fig. 4: (Colour on-line) The average domain size R as a function of time t for a 50:50 critical mixture. The upper black curve is the pure 2D case showing an $\alpha = 1/2$ scaling, and the lower red curve is the quasi-2D case when $L_z = 40$ showing a distinct $\alpha = 1/3$ scaling. The inset shows the zoomed in portion with different box heights in the z -direction as in fig. 3.

covers about one decade in time, which is similar to that previously shown in the literature [18]. A larger system size $L_x \times L_y = 200 \times 200$ also produced the same scaling for the pure 2D case, which demonstrates that finite-size effects are small. However, we present here only the results for the 80×80 system in 2D, because this is the system size studied for the quasi-2D case with a bulk fluid, which requires a large amount of particles in 3D.

In fig. 4, we show the result for a component ratio of 50:50 (critical mixture). In this case, the growth exponent for the pure 2D case is less obvious owing to rapid coarsening of the domains. However, by simulating a bigger system 200×200 with the same areal density, an $\alpha = 1/2$ exponent is indeed obtained. Similar to the off-critical case, the growth of the domains is slowed down by the addition of solvent and the exponent is reduced to $\alpha = 1/3$. These results indicate that solvent is responsible for slowing down the growth dynamics.

The observed exponent $\alpha = 1/2$ in pure 2D systems can be explained in terms of the Brownian coagulation mechanism [12]. From dimensional analysis, the 2D diffusion coefficient of the domain is given by $D_2 \sim k_B T / \eta$, where η is the film 2D viscosity. Using the relation

$$R^2 \sim D_2 t \sim (k_B T / \eta) t, \quad (3)$$

we find $R \sim t^{1/2}$. For 3D systems, on the other hand, the diffusion coefficient of the droplet is inversely proportional to its size, $D_3 \sim 1/R$, a well-known Stokes-Einstein relation. Hence the Brownian coagulation mechanism in 3D

gives rise to an exponent $\alpha = 1/3$. (In general, the exponent is $\alpha = 1/d$, where d is the space dimension.) The change in the exponent from $\alpha = 1/2$ to $1/3$ due to the addition of solvent implies the crossover from 2D to 3D behaviors of the phase separation dynamics even though the lateral coarsening takes place only within the 2D geometry¹. Therefore it is necessary to examine the size dependence of the domain diffusion coefficient in quasi-2D systems. This can be calculated by tracking the mean-squared displacement of domains of various radii. The equivalent information can be more efficiently obtained by calculating the two-particle longitudinal coupling diffusion coefficient in a single component film rather than in a binary system. This is described in the next section.

Correlated diffusion. – Consider a pair of particles separated by a 2D vector \mathbf{s} , undergoing diffusion in the liquid film. The two-particle mean squared displacement is given by [21]

$$\langle \Delta s_i^k \Delta s_j^l \rangle = 2D_{ij}^{kl}(\mathbf{s})t, \quad (4)$$

where Δs_i^k is the displacement of the particle k ($= 1, 2$) along the axis i ($= x, y$), D_{ij}^{kl} is the diffusion tensor giving self-diffusion when $k = l$ and the coupling between them when $k \neq l$. The x -axis is defined along the line connecting a pair of particles 1 and 2, *i.e.*, $\mathbf{s} = s\hat{x}$. Hence, we have $D_{xy}^{12} = 0$ by symmetry. The longitudinal coupling diffusion coefficient, $D_L^c(\mathbf{s}) = D_{xx}^{12}(s\hat{x})$, gives the coupled diffusion along the line of centers of the particles. We first describe the analytical expression of $D_L^c(\mathbf{s})$ based on the Saffman and Delbrück (SD) theory which was originally developed for protein diffusion in membranes [15].

Since the calculation of the diffusion coefficient in a pure 2D system is intractable due to Stokes paradox, SD circumvented this problem by taking into account the presence of the solvent with 3D viscosity η_s above and below the membrane. Suppose a point force \mathbf{f} directed along the plane of the film lying in the xy -plane acts at the origin. Then we seek for the velocity $\mathbf{v}(\mathbf{s})$ induced at the position \mathbf{s} . According to the SD theory, it is given in Fourier space, $\mathbf{v}[\mathbf{q}] = \int d\mathbf{s} e^{-i\mathbf{q}\cdot\mathbf{s}} \mathbf{v}(\mathbf{s})$, as [15,21,22]

$$v_i[\mathbf{q}] = G_{ij}^{\text{SD}}[\mathbf{q}] f_j = \frac{1}{\eta q (q + \nu)} \left(\delta_{ij} - \frac{q_i q_j}{q^2} \right) f_j, \quad (5)$$

where G^{SD} is the 2D film analog of the Oseen tensor. In the above, the SD length is defined by $\nu^{-1} = \eta / 2\eta_s$.

For over damped dynamics, we can use the Einstein relation to relate the diffusion tensor D_L^c to G_{ij}^{SD} [21]. After converting $G_{ij}^{\text{SD}}[\mathbf{q}]$ into real space, we obtain

$$\begin{aligned} D_L^c(\mathbf{s}) &= k_B T G_{xx}^{\text{SD}}(s\hat{x}) \\ &= \frac{k_B T}{4\pi\eta} \left[\frac{\pi \mathbf{H}_1(\nu s)}{\nu s} - \frac{\pi Y_1(\nu s)}{\nu s} - \frac{2}{(\nu s)^2} \right], \end{aligned} \quad (6)$$

¹We note that the LS mechanism shows an exponent of $\alpha = 1/3$ for both 2D and 3D. Thus our simulations are still in the early stage of the coarsening dynamics.

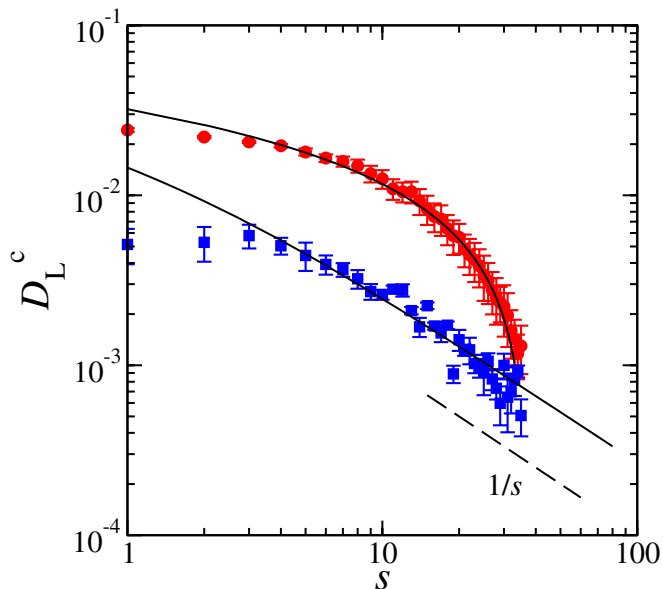


Fig. 5: (Colour on-line) Longitudinal coupling diffusion D_L^c as a function of particle separation s . The upper circles are data for the pure 2D case. The lower squares correspond to the case with solvent when $L_z = 40$. The upper solid line is the fit by eq. (7), and the lower solid line is the fit by eq. (6). The dashed line shows the $1/s$ -dependence.

where \mathbf{H}_1 and Y_1 are the Struve function and the Bessel function of the second kind, respectively. At short distances $s \ll \nu^{-1}$, the asymptotic form of the above expression becomes

$$D_L^c(s) \approx \frac{k_B T}{4\pi\eta} \left[\ln\left(\frac{2}{\nu s}\right) - \gamma + \frac{1}{2} \right], \quad (7)$$

where $\gamma = 0.5772 \dots$ is Euler's constant. At large inter-particle separations $s \gg \nu^{-1}$, on the other hand, eq. (6) reduces to

$$D_L^c(s) \approx \frac{k_B T}{2\pi\eta\nu s} = \frac{k_B T}{4\pi\eta_s s}, \quad (8)$$

showing the asymptotic $1/s$ decay which reflects the 3D nature of this limit. Notice that eq. (8) depends only on the solvent viscosity η_s but not on the film viscosity η any more.

In fig. 5, we plot the measured longitudinal coupling diffusion coefficient D_L^c as a function of the 2D distance s . In these simulations, we have worked only with single-component films with the same system sizes and number of particles as those used for the phase separation simulations. We have also taken the average over 20 independent trials. In the pure 2D case without any solvent, D_L^c shows a logarithmic dependence on s . This is consistent with eq. (7) obtained when the coupling between the film and the solvent is very weak so that the film can be regarded almost as a pure 2D system. Using eq. (7) as an approximate expression, we get from the fitting $k_B T/4\pi\eta \approx 0.89 \times 10^{-2}$ and $\nu^{-1} \approx 20$. In an ideal case, the SD length should diverge due to the absence of solvent.

The obtained finite value for ν^{-1} is roughly set by half of the system size in the simulation.

When we add solvent ($L_z = 40$), the D_L^c is decreased and no longer behaves logarithmically. In this case, we use the full expression eq. (6) for the fitting, and obtained $k_B T/4\pi\eta \approx 1.35 \times 10^{-2}$ and $\nu^{-1} \approx 1$. In the above two fits we have neglected the first two points as they lie outside the range of validity, $s \gg 1$, of eq. (6) [21]. Since $\nu^{-1} \approx 1$ when the solvent is present, the data shown in fig. 5 are in the crossover region, $s \gtrsim \nu^{-1}$, showing an approach towards the asymptotic $1/s$ -dependence as in eq. (8). Hence we conclude that the solvent brings in the 3D hydrodynamic property to the diffusion in films. This is the reason for the 3D exponent $\alpha = 1/3$ in the phase separation dynamics, and justifies that it is mainly driven by the Brownian coagulation mechanism.

In our simulations the film and the solvent have very similar viscosities. This sets the SD length scale to be of the order of unity, which is consistent with the value $\nu^{-1} \approx 1$ obtained from the fitting. As explained above, the fit also provides the 2D film viscosity as $\eta \approx 6$, and hence we obtain as $\eta_s \approx 3$. This value is in reasonable agreement with the value $\eta_s \approx 1$ calculated in ref. [23] by using the reverse Poiseuille flow method. The reason for the slightly higher value of η_s in our simulations is that the tracer particles are of the same size as the film particles. This may lead to an underestimation of the correlated diffusion coefficient. In real biomembranes sandwiched by water, however, the value of the SD length is much larger than the lipid size, and is in the order of micron scale [15]. Hence the 3D nature of hydrodynamics can be observed only for large enough domains observed under optical microscopes [5].

Discussion. – Several points merit further discussion.

The growth exponents obtained from our simulations for critical mixtures are the same for the off-critical case, namely $\alpha = 1/2$ without solvent and $\alpha = 1/3$ with solvent. A previous DPD study by Laradji and Kumar on phase separation dynamics of two-component membranes (both critical and off-critical cases) used a coarse-grained model for the membrane lipids [18]. In their model, the self-assembly of the bilayer in the presence of solvent is naturally taken into account. The exponent for the off-critical case $\alpha = 1/3$ is the same as that obtained in our study, although they attributed this value to the LS mechanism. For critical mixtures in the presence of solvent, they obtained a different value $\alpha = 1/2$. A suitable explanation for this exponent was not given in their paper.

As a related experimental work, the diffusion of tracer particles embedded in a soap film was recently reported [24]. When the diameter of the tracer particles is close to the thickness of the soap film, the system shows a 2D behavior. On the other hand, if the particle diameter is much smaller than the soap film thickness, it executes a 3D motion. On systematically increasing the soap film thickness, they identified a transition from 2D to 3D nature. In this paper, we have demonstrated the

analogue for a 2D liquid film-solvent system using DPD simulations.

In the SD theory, the bulk fluid is assumed to occupy an infinite space above and below the membrane. The situation is altered when the solvent and the membrane are confined between two solid walls [22]. If the distance H between the membrane and the wall is small enough, we are in a situation similar to that described by Evans and Sackmann [25]. The Oseen tensor G^{ES} in this case is defined through the relation [26],

$$v_i[\mathbf{q}] = G_{ij}^{\text{ES}}[\mathbf{q}]f_j = \frac{1}{\eta(q^2 + \kappa^2)} \left(\delta_{ij} - \frac{q_i q_j}{q^2} \right) f_j, \quad (9)$$

where the new length scale is defined as $\kappa^{-1} = \sqrt{\eta H / 2\eta_s}$. Notice that κ^{-1} is the geometric mean of ν^{-1} and H [27]. Following the same procedure as in the previous section, the longitudinal coupling diffusion coefficient can be obtained as

$$D_L^c(s) = \frac{k_B T}{2\pi\eta} \left[\frac{1}{(\kappa s)^2} - \frac{K_1(\kappa s)}{\kappa s} \right], \quad (10)$$

where K_1 is a modified Bessel function of the second kind. At short distances $s \ll \kappa^{-1}$, we have

$$D_L^c(s) \approx \frac{k_B T}{4\pi\eta} \left[\ln \left(\frac{2}{\kappa s} \right) - \gamma + \frac{1}{2} \right], \quad (11)$$

which is almost identical to eq. (7) except ν is replaced now by κ . At long distances $s \gg \kappa^{-1}$, on the other hand, we get

$$D_L^c(s) \approx \frac{k_B T}{2\pi\eta\kappa^2 s^2} = \frac{k_B T H}{4\pi\eta_s s^2}, \quad (12)$$

which exhibits a $1/s^2$ -dependence. This is in contrast to eq. (8). Following a similar scaling argument as before, we predict that, in the presence of solid walls, the domain growth exponent should be $\alpha = 1/4$ within the Brownian coagulation mechanism. In biological systems, the above model with solid walls can be relevant because the cell membranes are strongly anchored to the underlying cytoskeleton, or are tightly adhered to other cells.

In summary, we have shown that the bulk fluid has a significant effect on the phase separation dynamics of thin liquid films through a simple quasi-2D simulation model. We have demonstrated the change in the growth exponents from 2D to 3D by the addition of bulk fluid. This is further justified by the two-particle correlation studies, which showed that the longitudinal coupling diffusion coefficient changes from a logarithmic dependence for the pure 2D case to an algebraic one for the quasi-2D case. Future directions include investigating the role of out-of-plane fluctuations and the effect of boundary walls on the phase separation.

This work was supported by KAKENHI (Grant-in-Aid for Scientific Research) on Priority Area ‘‘Soft Matter

Physics’’ and Grant No. 21540420 from the Ministry of Education, Culture, Sports, Science and Technology of Japan.

REFERENCES

- [1] SIMONS K. and IKONEN E., *Nature*, **387** (1997) 569.
- [2] VEATCH S. L. and KELLER S. L., *Biochim. Biophys. Acta*, **1746** (2005) 172.
- [3] HONERKAMP-SMITH A. R., CICUTA P., COLLINS M., VEATCH S. L., SCHICK M., DEN NIJS M. and KELLER S. L., *Biophys. J.*, **95** (2008) 236.
- [4] VEATCH S. L., CICUTA P., SENGUPTA P., HONERKAMP-SMITH A., HOLOWKA D. and BAIRD B., *J. Chem. Biol.*, **3** (2008) 287.
- [5] CICUTA P., KELLER S. L. and VEATCH S. L., *J. Phys. Chem. B*, **111** (2007) 3328.
- [6] YANAGISAWA M., IMAI M., MASUI T., KOMURA S. and OHTA T., *Biophys. J.*, **92** (2007) 115.
- [7] BRAY A. J., *Adv. Phys.*, **51** (2002) 481.
- [8] BINDER K. and STAUFFER D., *Phys. Rev. Lett.*, **33** (1974) 1006.
- [9] LIFSHITZ E. M. and PITAEVSKII L. P., *Physical Kinetics* (Pergamon Press, Oxford) 1981.
- [10] FURUKAWA H., *Physica A*, **204** (1994) 237.
- [11] SIGGIA E. D., *Phys. Rev. A*, **20** (1979) 595.
- [12] MIGUEL M. S., GRANT M. and GUNTON J. D., *Phys. Rev. A*, **31** (1985) 1001.
- [13] OSSADNIK P., GYURE M. F., STANLEY H. E. and GLOTZER S. C., *Phys. Rev. Lett.*, **72** (1994) 2498.
- [14] GONNELLA G., ORLANDINI E. and YEOMANS J. M., *Phys. Rev. E*, **59** (1999) R4741.
- [15] SAFFMAN P. G. and DELBRÜCK M., *Proc. Natl. Acad. Sci. U.S.A.*, **72** (1975) 3111; SAFFMAN P. G., *J. Fluid Mech.*, **73** (1976) 593.
- [16] GROOT R. D. and WARREN P. B., *J. Chem. Phys.*, **107** (1997) 4423.
- [17] ESPANOL P. and WARREN P., *Europhys. Lett.*, **30** (1995) 191.
- [18] LARADJI M. and KUMAR P. B. S., *Phys. Rev. Lett.*, **93** (2004) 198105; *J. Chem. Phys.*, **123** (2005) 224902.
- [19] RAMACHANDRAN S., KUMAR P. B. S. and LARADJI M., *J. Chem. Phys.*, **129** (2008) 125104; *J. Phys. Soc. Jpn.*, **78** (2009) 041006.
- [20] ALTENHOFF A. M., WALTHER J. H. and KOUMOUTSAKOS P., *J. Comput. Phys.*, **225** (2007) 1125.
- [21] OPPENHEIMER N. and DIAMANT H., *Biophys. J.*, **96** (2009) 3041.
- [22] INAURA K. and FUJITANI Y., *J. Phys. Soc. Jpn.*, **77** (2008) 114603.
- [23] PAN W., FEDOSOV D. A., KARNIADAKIS G. E. and CASEWELL B., *Phys. Rev. E*, **78** (2008) 046706.
- [24] PRASAD V. and WEEKS E. R., *Phys. Rev. Lett.*, **102** (2009) 178302.
- [25] EVANS E. and SACKMANN E., *J. Fluid Mech.*, **194** (1988) 553.
- [26] SEKI K., KOMURA S. and IMAI M., *J. Phys: Condens. Matter*, **19** (2007) 072101.
- [27] STONE H. and AJDARI A., *J. Fluid Mech.*, **369** (1998) 151.